Navigation of an n-link Revolute Robotic Arm via Hierarchal Landmarks

Ravinesh Chand †,*, Sandeep A. Kumar ‡ and Ronal P. Chand †

2021 3rd Novel Intelligent and Leading Emerging Sciences Conference (NILES) | 978-1-6654-2157-7/21/$31.00 ©2021 IEEE | DOI: 10.1109/NILES53778.2021.9600539

***Abstract*—This paper presents a dynamic n-link revolute robotic arm that can perform a sequence of tasks and navigate via hierarchal landmarks to its target. The stability condition with multiple Lyapunov functions for switched systems is considered. The multiple Lyapunov functions are formulated from the Lyapunov-based Control Scheme (LbCS) as a tool for analyzing Lyapunov stability. A new set of switched nonlinear, time-invariant, continuous, and stabilizing velocity controllers of the proposed R^n robotic arm are developed.**

***Index Terms*—revolute, n-link robotic arm, hierarchal landmark, velocity controllers**

I. Introduction

To help increase productivity and meet consumer demands while lowering overall costs, industries have to continuously find ways not only to keep pace with the demand for products but also finding skilled workers to get tasks done. As such, industries have been actively researching upon adopting different forms of robotic technology. A number of robotic mechanical systems such as aerial and ground vehicles [1]–[3], car-like [4], tractor-trailer [5], swarms [6], [7], and mobile manipulators [8]–[10] have been researched. To attain stable and controlled motions of robotic systems recently, the method of Lyapunov-based Control Scheme (LbCS) has been utilized, as demonstrated in [11], [12], and [8]. The landmark technique, including hierarchal landmarks, has also been used in studies such as [13], [14] and [15] to guide a robot to the desired goal. In the industrial sector, the robotic arm is commonly utilized to assist in improving production capacity of manufacturing companies [16], [17]. Depending on the application, a robotic arm can either be fixed to a position as anchored [12], or used as an active component of mobile manipulators as unanchored [5]. According to [14], robotic arms can be classified by the type of link of the arm, the two common types being prismatic and revolute joints.

A quick glance at the past two decades reveals that researchers initially focussed on 2-link [16] and 3-link manipulators [18]. Later, researchers gradually and confidently introduced additional links to the robotic arm systems, including 4-link [12], 5-link [19], and 6-link robotic arms [20]. However, a literature search also reveals that an n-link robotic arm has not been given much attention in terms of research.

The lack of attention given by researchers to study the effectiveness of a generalised version n-link robotic arm serves as the motivation for this research. This paper, using LbCS [21]–[23], aims to develop the velocity controllers of an n-link revolute robotic arm (R^n), which navigates to its target via hierarchal landmarks. This method can offer valuable contributions in real-life applications such as health care, manufacturing, and assembly line production.

The main contributions of this paper are:

1) a new dynamic n-link robotic arm that can track multiple targets and accomplish $h+1$ tasks, given h hierarchal landmarks.
2) Navigation of an R^n robotic arm through hierarchal landmarks.
3) switched nonlinear, time-invariant, continuous, and stabilizing velocity controllers of R^n robotic arm.

In Section 2, the system modeling of an n-link revolute robotic arm is shown. Section 3 discusses the problem that this paper will address via landmarks for an n-link robot arm. In Section 4, the switched velocity controllers are derived from multiple Lyapunov functions. The stability analysis of the n-link robot arm is given in Section 5. Then, in Section 6, the simulation results are presented, followed by conclusion and future works in Section 7.

II. System Modeling

The research considers an n-link revolute robotic arm, having n rotational joints in the z_1z_2-plane as

† School of Mathematical & Computing Sciences, Fiji National University, Suva, Fiji.
‡ School of Information Technology, Engineering, Mathematics & Physics, The University of the South Pacific, Suva, Fiji.
*Corresponding author email: ravinesh.c@fnu.ac.fj

978-1-6654-2157-7/21/$31.00 ©2021 IEEE

Authorized licensed use limited to: University of the South Pacific. Downloaded on February 08,2022 at 03:21:16 UTC from IEEE Xplore. Restrictions apply.

shown in Figure 1. The articulated arm consists of n rigid links which are connected via revolute joints and the n^{th} link has an end-effector. With the help

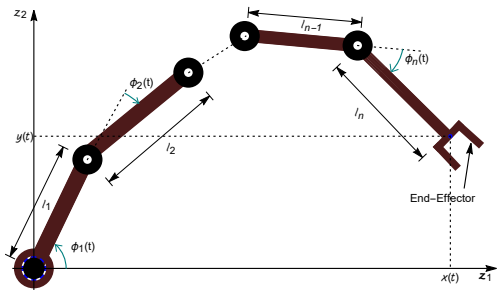

Fig. 1. Schematic representation of a n-link Revolute Manipulator.

of the Figure 1, it is assumed that:

i. the planar R^n manipulator is anchored at the origin;
ii. the length of the i^{th} revolute link is l_i with an angular position $\phi_i(t)$ at time t with the horizontal z_1 axis;
iii. the last link (link n) has the length l_n with an angular position $\phi_n(t)$ at time t; and
iv. the coordinates of the gripper are $(x(t), y(t))$ and given as:

$$\begin{aligned} x(t) =& \sum_{i=1}^{n} l_i \cos\left(\sum_{k=1}^{i} \phi_k(t)\right), \\ y(t) =& \sum_{i=1}^{n} l_i \sin\left(\sum_{k=1}^{i} \phi_k(t)\right). \end{aligned} \tag{1}$$

To describe the motion of the n-link revolute robotic arm with an end-effector, a system of differential equations is constructed. The position of the end-effector of the n-link robot arm at $t \geq 0$ is denoted as $\boldsymbol{x} = (x(t), y(t)))$ with an orientation angle of $\phi_n = \phi_n(t)$. Let the angular orientation of the i^{th} link be $\phi_i = \phi_i(t)$ for $i \in \{1, 2, 3..., n\}$. The kinematic model of the n-link robot arm, upon suppressing t, is as follows:

$$\left.\begin{aligned} \dot{x} =& -\sum_{i=1}^{n} v_i \left(y - \sum_{j=1}^{i-1} l_j \sin\left(\sum_{k=1}^{j} \phi_k\right)\right), \\ \dot{y} =& \sum_{i=1}^{n} v_i \left(x - \sum_{j=1}^{i-1} l_j \cos\left(\sum_{k=1}^{j} \phi_k\right)\right), \\ \dot{\phi}_i =& v_i. \end{aligned}\right\} \tag{2}$$

At $t \geq 0$, let $\phi_i'(t)$ be the instantaneous angular velocity of the i^{th} revolute link with the end-effector. Thus, a system of first-order ODEs for the i^{th} revolute link is obtained as:

$$\phi_i'(t) = v(t), \tag{3}$$

assuming the initial conditions at $t = t_0 \geq 0$ as $x_0 := x(t_0)$, $y_0 := y(t_0)$, $\phi_{i0} := \phi_i(t_0)$. Let $\boldsymbol{x}_0 = (x_0, y_0)$. Suppressing t, the state vector is given as $\mathbf{x} := (x, y, \phi_1, \phi_2, \ldots, \phi_n) \in \mathbb{R}^{n+2}$. Also, let $\mathbf{x}_0 := \mathbf{x}(t_0) := (x_0, y_0, \phi_{1_0}, \phi_{2_0}, \ldots, \phi_{n_0}) \in \mathbb{R}^{n+2}$. If the instantaneous velocity v_i has the state feedback law of the form

$$v_i(t) := -\varphi_i f_i(\mathbf{x}(t)),$$

for $i \in \{1, 2, 3, \ldots, n\}$, for some scalars φ_i and some functions $f_i(\mathbf{x}(t))$, to be constructed appropriately later, and if we define $\mathbf{F}(\mathbf{x}) := (-\varphi_1 f_1(\mathbf{x}), -\varphi_2 f_2(\mathbf{x}), \ldots, -\varphi_n f_n(\mathbf{x})) \in \mathbb{R}^n$, then the n-link robotic arm is represented by

$$\dot{\mathbf{x}} = \mathbf{F}(\mathbf{x}), \quad \mathbf{x}(t_0) = \mathbf{x}_0. \tag{4}$$

III. Problem Statement

In the industrial sector, the introduction of robotic arms has eased repetitive assembly line works. Unlike human labour, robotic arms can operate under immense conditions, hence contributing to an improved production capacity of manufacturing companies [16]. While studies such as [16], [18], [19], and [20] utilized 2-link, 3-link, 5-link, and 6-link mechanisms, respectively, the robotic arm proposed in this paper is a generalized version that is more dynamic, comprising of n-links. The proposed robotic arm will have the added advantage of performing a sequence of tasks with relative ease.

Consider a workspace of an n-link revolute manipulator with predefined $h \in \mathbb{N}$ hierarchal landmarks. Assume that the locations of the $h \in \mathbb{N}$ hierarchal landmarks, λ_p for $p \in \{1, 2, \ldots, h\}$, have been predetermined. The end-effector of the n-link revolute manipulator has to navigate to the target location via the h hierarchal landmarks. Thus, the robotic arm manages to perform a sequence of tasks in one complete cycle.

Definition 1. The p^{th} landmark λ_p, for $p = 1, 2, ..., h$, is a disk with center $\boldsymbol{x}_{\lambda_p} = (x_{\lambda_p}, y_{\lambda_p})$ and radius r_{λ_p}. The set λ_p is defined as:

$$\lambda_p = \{(z_1, z_2) \in \mathbb{R}^2 : (z_1 - x_{\lambda_p})^2 + (z_2 - y_{\lambda_p})^2 \leq r_{\lambda_p}^2\}.$$

Definition 2. The ultimate target for a n-link robotic arm is a disk with the center $\boldsymbol{x}_\rho = (a, b)$ and radius r_ρ. It is described as the set:

$$\rho := \{(z_1, z_2) \in \mathbb{R}^2 : (z_1 - a)^2 + (z_2 - b)^2 \leq r_\rho^2\}.$$

Authorized licensed use limited to: University of the South Pacific. Downloaded on February 08,2022 at 03:21:16 UTC from IEEE Xplore. Restrictions apply.

The target $\boldsymbol{x}_\rho$ will be considered as an additional landmark, that is, $\lambda_{h+1} = \boldsymbol{x}_\rho$.

Definition 3. The distance, δ_{λ_p}, between the initial position of the robot end-effector, $\boldsymbol{x}_0$, and the pth landmark, is given by:

$$\delta_{\lambda_p} = \left\| \boldsymbol{x}_0 - \boldsymbol{x}_{\lambda_p} \right\|, \tag{5}$$

where $p \in \{1, 2, 3, ..., h+1\}$.

It is further assumed that

$$\delta_{\lambda_1} < \delta_{\lambda_2} < \delta_{\lambda_3} < ... < \delta_{\lambda_{h+1}}.$$

Definition 4. The equilibrium point for the n^{th} link is defined as:

$$\mathbf{x}_e := (a, b, \phi_1, \phi_2, \ldots, \phi_n) \in \mathbb{R}^{n+2},$$

where ϕ_i represents the final orientation angle of the i^{th} revolute link for $i \in \{1, 2, \ldots, n\}$.

IV. Velocity Controllers

To ensure that the end-effector of the n-link robotic arm maneuvers to the p^{th} hierarchal landmark, let the attractive potential be:

$$A_p(\boldsymbol{x}) = \frac{1}{2} \left\| \boldsymbol{x} - \boldsymbol{x}_{\lambda_p} \right\|^2. \tag{6}$$

To ensure that the end-effector converges to its equilibrium position, radically unbounded functions about the target are utilized. Let an auxiliary function be:

$$C(\boldsymbol{x}) = \frac{1}{2} \left\| \boldsymbol{x} - \boldsymbol{x}_\rho \right\|^2. \tag{7}$$

All the singularities caused by the anchored arm's geometric arrangement need to be accounted for. Link 1 of the anchored arm cannot rotate fully to the horizontal surface on which it is mounted on, when rotating both clockwise and counterclockwise. The singularities of link 1 arise when $\phi_1 \in \{\theta, \pi - \theta\}$. To avoid the singularities of the first link of the revolute arm, the following functions are introduced:

$$S_1 = \theta - \phi_1 \text{ and } S_2 = \pi - \theta - |\phi_1|$$

Likewise, link 2 cannot fully fold with link 1 while rotating both clockwise and counterclockwise. This singularity of link 2 arise when $\phi_2 = |\phi_{2_{max}}|$. The same singularity arises for other revolute links. Thus, it could be generalized as $\phi_i = |\phi_{i_{max}}|$ for $i \in \{2, 3, \ldots, n\}$.
To avoid interior singularities of the other revolute links, consider the function:

$$S_{i+1} = \phi_{i_{max}} - |\phi_i|, \text{ for } i = \{2, 3, .., n\}.$$

By evaluating the value of multiple Lyapunov functions during the activation period of each subsystem, a new Lyapunov stability condition will be presented. The value of the multiple Lyapunov functions will be evaluated at the starting points or the end points. Let ξ, η_p and τ_i be positive real numbers, and let $\delta = \left\| x - x_{\lambda_p} \right\|$. For $i \in \{1, 2, 3, ..., n\}$, define a family of Lyapunov functions of the form,

$$L_p(\mathbf{x}) = C(\boldsymbol{x}) \left(\xi + \eta_p A_p(\boldsymbol{x}) + \sum_{i=1}^{n+1} \frac{\tau_i}{S_i} \right), \tag{8}$$

which will operate according to the switching rule

$$p = \begin{cases} 1 & 0 \le \delta < \delta_{\lambda_1} \\ 2 & \delta_{\lambda_1} \le \delta < \delta_{\lambda_2} \\ \vdots & \\ h+1 & \delta_{\lambda_h} \le \delta \le \delta_{\lambda_{h+1}} \end{cases} \tag{9}$$

Along a trajectory of system (4), there is

$$\dot{L}_p(\mathbf{x}) = \sum_{i=1}^{n} f_{i_p} v_i, \tag{10}$$

where

$$f_{i_p}(\mathbf{x}) = \frac{\partial L_p(\mathbf{x})}{\partial \phi_i}. \tag{11}$$

Let there be a scalar $\varphi_i > 0$, then the velocity controller of system (4) is

$$v_i = -\varphi_i f_{i_p}. \tag{12}$$

V. Stability Analysis

The Lyapunov function $L_p(\mathbf{x})$, for $p = \{1, 2, \cdots, h+1\}$, is positive over the domain

$$D\big(L_p(\mathbf{x})\big) := \Big\{ \mathbf{x} \in \mathbb{R}^{n+2} : S_i > 0, \, \forall \, i = \{1, 2, 3, \ldots, n+1\} \Big\}.$$

With respect to system (2),

$$\dot{L}_p(\mathbf{x}) = -\sum_{i=1}^{n} \varphi_i {f_{i_p}}^2 \le 0,$$

$\forall \mathbf{x} \in D\big(L_p(\mathbf{x})\big)$. At the target, where $(x, y) = (a, b)$, the instantaneous velocity, v_i is zero because $f_{i_p} = 0$. This implies that the end-effector of the n-link arm is at the target position. The target position and the final angular positions of the n-links with horizontal axis are components of an equilibrium point $\mathbf{x}_e$ of the system. It is easy to see that $L_p(\mathbf{x}_e) = 0$, $L_p(\mathbf{x}) > 0 \; \forall \; \mathbf{x} \neq \mathbf{x}_e$ and $\dot{L}_p(\mathbf{x}) \le 0$. The system has a simple switching sequence $\mathbb{S} = (x_0, y_0) : (p_0, t_0), (p_1, t_1)$

Authorized licensed use limited to: University of the South Pacific. Downloaded on February 08,2022 at 03:21:16 UTC from IEEE Xplore. Restrictions apply.

for $p = 1, \ldots, h+1$, from which the trajectory is obtained:

$$\mathbf{x}_{\mathbb{S}}(\cdot) := \Big\{(p_0, t_0) : \dot{\mathbf{x}} = \mathbf{F}_{p_0}(\mathbf{x}(t), t), \quad p = 1, \ldots, h+1,\ t_0 \leq t < t_1\Big\}.$$

Thus, $L_p(\mathbf{x})$ are monotonically non-increasing on $\mathcal{I}(\mathbb{S}|p)$. Hence, for $\mathbb{S}$ and for all p, L_p are Lyapunov-like functions. Accordingly, by Branicky's Theorem 2.3 [24], the system is stable in the sense of Lyapunov.

VI. Simulation Results

Computer simulations were generated using Wolfram Mathematica 11.2 software. To achieve the desired results, a number of sequential Mathematica commands were executed. Before the algorithm is executed, the values of the convergence, system singularities and restriction avoidance parameters have to be stated using the brute-force technique.The number and positions of the hierarchal landmarks, and initial state of the R^n robotic arm have to be defined. The system was numerically simulated using the RK4 method (Runge-Kutta Method). At $t = 0$, the initial positions $(x_0(0), y_0(0))$, and orientations $\phi_i(0)$ were generated. The following example shows the simulation results of a 6-link robotic arm.

A. Example

In this example, a 6-link robotic arm anchored at (5, 5) is considered. The arm should maneuver through each of the four hierarchal landmarks in one sequence. All the links of the arm has a length of 4.2. The coordinates of the target is (4, 28.5), while the coordinates of the four landmarks are $(x_{\lambda_1}, y_{\lambda_1}) = (26, 10)$, $(x_{\lambda_2}, y_{\lambda_2}) = (24, 17)$, $(x_{\lambda_3}, y_{\lambda_3}) = (19, 23)$ and $(x_{\lambda_4}, y_{\lambda_4}) = (11, 27)$ respectively. The target attraction parameter is $\xi = 0.001$, while the landmark attraction parameters are $\eta_1 = \eta_2 = 0.05$, $\eta_3 = 0.5$, and $\eta_4 = \eta_5 = 0.06$. The initial orientations of the revolute links are $\phi_{1_0} = \frac{\pi}{2}, \phi_{2_0} = -\frac{5\pi}{6}, \phi_{3_0} = \phi_{5_0} = \frac{7\pi}{9}$ and $\phi_{4_0} = \phi_{6_0} = -\frac{7\pi}{9}$. The convergence parameter for the revolute link orientation angle is $\varphi_i = 0.05$ for $i \in \{1, 2, \ldots, 6\}$, while the parameter for restriction on orientation of the revolute links is $\tau_i = 0.00001$ for $i \in \{1, 2, \ldots, 7\}$. The revolute link 1 limitation angle is $\theta = \frac{\pi}{7}$ and the maximum possible revolute link orientation angle is $\phi_{i_{max}} = \frac{8\pi}{9},\ i \in \{2, 3, \ldots, 6\}$.

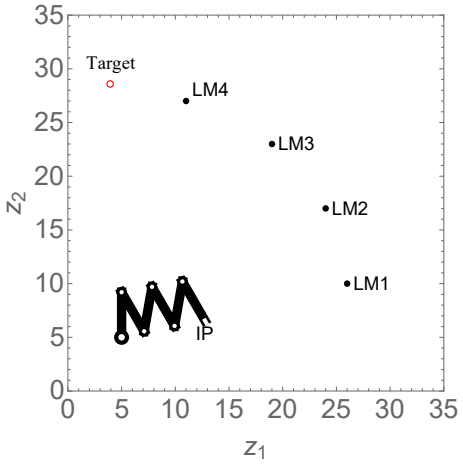

Fig. 2. The initial position (IP), initial orientation, the positions of four landmarks labelled as LM1, LM2, LM3, and LM4 and target of a 6-link revolute arm.

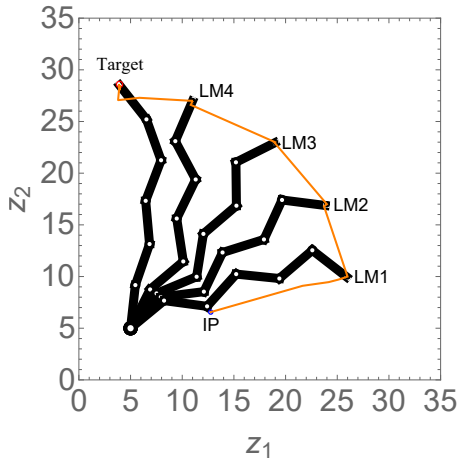

Fig. 3. Positions and orientations of the links at time $t = 20, 25, 30, 35,$ and 500.

VII. Conclusion

Robotic arm systems have eased repetitive assembly line works in our industry sector. In this paper, a set of nonlinear, time-invariant, and switched stabilizing velocity controllers of an anchored n-link revolute robotic arm has been established to navigate to its ultimate target via hierarchal landmarks while observing system restrictions and limitations. From the authors' point of view, this is the first time such stabilizing switched velocity-based controllers are derived for an n-link revolute robotic arm in Lyapunov's sense.

This has provided a solution to the common prob-

Authorized licensed use limited to: University of the South Pacific. Downloaded on February 08,2022 at 03:21:16 UTC from IEEE Xplore. Restrictions apply.

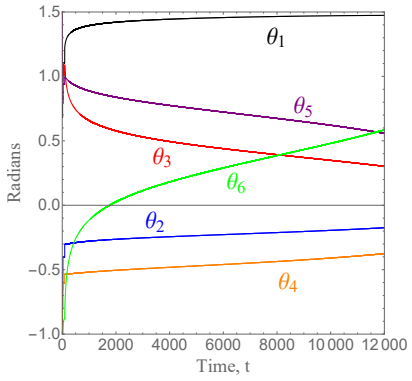

Fig. 4. Orientations of the revolute links.

lem tagged to robotic arms that require certain tasks that need to be addressed in an hierarchal order. For instance, robotics arms in automated assembly line could perform a number of tasks which are in hierarchal order. As future work, switched velocity controllers will be considered for an n-link prismatic robotic arm.

References

[1] Sandeep A Kumar, Jito Vanualailai, Bibhya Sharma, and Avinesh Prasad. Velocity controllers for a swarm of unmanned aerial vehicles. *Journal of Industrial Information Integration*, 22:100198, 2021.

[2] Jito Vanualailai, Ashna Sharan, and Bibhya Sharma. A swarm model for planar formations of multiple autonomous unmanned aerial vehicles. In *2013 IEEE International Symposium on Intelligent Control (ISIC)*, pages 206–211, 2013.

[3] Amrita Devi, Jito Vanualailai, Sandeep A Kumar, and Bibhya Sharma. A cohesive and well-spaced swarm with application to unmanned aerial vehicles. In *2017 International Conference on Unmanned Aircraft Systems (ICUAS)*, pages 698–705. IEEE, 2017.

[4] Bibhya Sharma, Jai Raj, and Jito Vanualailai. Navigation of carlike robots in an extended dynamic environment with swarm avoidance. *International Journal of Robust and Nonlinear Control*, 28(2):678–698, 2018.

[5] Avinesh Prasad, Bibhya Sharma, Jito Vanualailai, and Sandeep A Kumar. A geometric approach to target convergence and obstacle avoidance of a nonstandard tractor-trailer robot. *International Journal of Robust and Nonlinear Control*, 30(13):4924–4943, 2020.

[6] Sandeep A Kumar, Jito Vanualailai, and Avinesh Prasad. Distributed velocity controllers of the individuals of emerging swarm clusters. In *2020 IEEE Asia-Pacific Conference on Computer Science and Data Engineering (CSDE)*, pages 1–6. IEEE, 2020.

[7] Sandeep A Kumar, Jito Vanualailai, Bibhya Sharma, Atin Chaudhary, and Vimi Kapadia. Emergent formations of a Lagrangian swarm of unmanned ground vehicles. In *2016 14th International Conference on Control, Automation, Robotics and Vision (ICARCV)*, pages 1–6. IEEE, 2016.

[8] Bibhya Sharma, Shonal Singh, Jito Vanualailai, and Avinesh Prasad. Globally rigid formation of n-link doubly nonholonomic mobile manipulators. *Robotics and Autonomous Systems*, 105:69–84, 2018.

[9] Sandeep A Kumar and Jito Vanualailai. A Lagrangian UAV swarm formation suitable for monitoring exclusive economic zone and for search and rescue. In *2017 IEEE Conference on Control Technology and Applications (CCTA)*, pages 1874–1879. IEEE, 2017.

[10] Avinesh Prasad, Bibhya Sharma, and Jito Vanualailai. A new stabilizing solution for motion planning and control of multiple robots. *Robotica*, 34(5):1071–1089, 2016.

[11] Bibhya Sharma, Jito Vanualailai, and Shonal Singh. Tunnel passing maneuvers of prescribed formations. *International Journal of Robust and Nonlinear Control*, 24(5):876–901, 2014.

[12] Bibhya Sharma, Jito Vanualailai, and Shonal Singh. Motion planning and posture control of multiple n-link doubly nonholonomic manipulators. *Robotica*, 35:1–25, March 2015.

[13] Avinesh Prasad, Bibhya Sharma, Jito Vanualailai, and Sandeep A Kumar. Stabilizing controllers for landmark navigation of planar robots in an obstacle-ridden workspace. *Journal of Advanced Transportation*, 2020.

[14] Avinesh Prasad, Bibhya Sharma, and Sandeep A Kumar. Strategic creation and placement of landmarks for robot navigation in a partially-known environment. In *2020 IEEE Asia-Pacific Conference on Computer Science and Data Engineering (CSDE)*, pages 1–6. IEEE, 2020.

[15] Sandeep A Kumar, Bibhya Sharma, Jito Vanualailai, and Avinesh Prasad. Stable switched controllers for a swarm of UGVs for hierarchal landmark navigation. *Swarm and Evolutionary Computation*, page 100926, 2021.

[16] Zhenli Lu, Aneesh Chauhan, Filipe Silva, and Luís Seabra Lopes. A brief survey of commercial robotic arms for research on manipulation. In *2012 IEEE Symposium on Robotics and Applications (ISRA)*, pages 986–991. IEEE, 2012.

[17] Bibhya Sharma, Jito Vanualailai, and Avinesh Prasad. A $d\phi$-strategy: Facilitating dual-formation control of a virtually connected team. *Journal of Advanced Transportation*, 2017:1–17, 2017.

[18] Thomas M Martinetz, Helge J Ritter, and Klaus J Schulten. Three-dimensional neural net for learning visomotor coordination of a robot arm. *IEEE transactions on neural networks*, 1(1):131–136, 1990.

[19] Jamshed Iqbal, R Ul Islam, and Hamza Khan. Modeling and analysis of a 6 DOF robotic arm manipulator. *Canadian Journal on Electrical and Electronics Engineering*, 3(6):300–306, 2012.

[20] Andrea Carron, Elena Arcari, Martin Wermelinger, Lukas Hewing, Marco Hutter, and Melanie N Zeilinger. Data-driven model predictive control for trajectory tracking with a robotic arm. *IEEE Robotics and Automation Letters*, 4(4):3758–3765, 2019.

[21] Sandeep A Kumar, Jito Vanualailai, and Bibhya Sharma. Lyapunov functions for a planar swarm model with application to nonholonomic planar vehicles. In *2015 IEEE Conference on Control Applications (CCA)*, pages 1919–1924. IEEE, 2015.

[22] Vishal Chand, Avinesh Prasad, Kaylash Chaudhary, Bibhya Sharma, and Samlesh Chand. A face-off - classical and heuristic-based path planning approaches. In *2020 IEEE Asia-Pacific Conference on Computer Science and Data Engineering (CSDE)*, pages 1–6, 2020.

[23] Sandeep A Kumar, Jito Vanualailai, and Bibhya Sharma. Navigation of carlike robots in an extended dynamic environment with swarm avoidance. *Mathematics in Computer Science*, 9(4):461–475, 2015.

[24] M. S. Branicky. Multiple Lyapunov fuctions and other analysis tools for switched and hybrid systems. *IEEE Transactions on Automatic Control*, 43(4):475–482, 1998.

Authorized licensed use limited to: University of the South Pacific. Downloaded on February 08,2022 at 03:21:16 UTC from IEEE Xplore. Restrictions apply.